

RSC Advances



This is an *Accepted Manuscript*, which has been through the Royal Society of Chemistry peer review process and has been accepted for publication.

Accepted Manuscripts are published online shortly after acceptance, before technical editing, formatting and proof reading. Using this free service, authors can make their results available to the community, in citable form, before we publish the edited article. This *Accepted Manuscript* will be replaced by the edited, formatted and paginated article as soon as this is available.

You can find more information about *Accepted Manuscripts* in the [Information for Authors](#).

Please note that technical editing may introduce minor changes to the text and/or graphics, which may alter content. The journal's standard [Terms & Conditions](#) and the [Ethical guidelines](#) still apply. In no event shall the Royal Society of Chemistry be held responsible for any errors or omissions in this *Accepted Manuscript* or any consequences arising from the use of any information it contains.



Journal Name

ARTICLE

Synthesis and self-assembly behavior of pH-responsive star-shaped POSS-(PCL-P(DMAEMA-co-PEGMA))₁₆ inorganic/organic hybrid block copolymer for the controlled intracellular delivery of doxorubicin

Received 00th January 20xx,

Accepted 00th January 20xx

DOI: 10.1039/x0xx00000x

www.rsc.org/

Lei Li^{1a}, Beibei Lu^{1a}, Qikui Fan^b, Jianning Wu^a, Lulu Wei^a, Jun Hou^d, Xuhong Guo^{a,c}, Zhiyong Liu^{a*}

In this work, a well-fined amphiphilic polyhedral oligomeric silsesquioxane (POSS) star-shaped inorganic/organic hybrid block copolymers with poly(ϵ -caprolactone)-poly(2-(dimethylamino)ethyl methacrylate)-co-poly(ethylene glycol) methacrylate (POSS-PCL-P(DMAEMA-co-PEGMA))₁₆ were synthesized with different PCL segments via thiol-ene click reaction, ring opening polymerization (ROP) and atom transfer radical polymerization (ATRP), which were confirmed by Fourier transforms infrared spectroscopy (FT-IR), proton nuclear magnetic resonance (¹H NMR), gel permeation chromatography (GPC), X-ray photoelectron spectroscopy (XPS) and thermogravimetric analysis (TGA). Subsequently, the polymers could self-assemble into micelles in aqueous solution, which were investigated by dynamic light scattering (DLS), ultraviolet-visible spectroscopy (UV-vis) and transmission electron microscopy (TEM). The pH-responsive self-assembly behavior of these triblock copolymers in water were investigated at different pH values of 5.0 and 7.4 for controlled doxorubicin release, the result indicated that the release rate of DOX could be effectively controlled by altering the pH, and the release of drug loading efficiency (DLE) were up to 82% (w/w). Furthermore, CCK-8 assays and confocal laser scanning microscopy (CLSM) against HeLa cells indicated that the micelles had no associated cytotoxicity, possessed good biodegradability and biocompatibility, and identified the location of the DOX in HeLa cells. The DOX-loaded micelles could easily enter the cells and produce the desired pharmacological action and minimize the side effect of free DOX. Moreover, these flexible micelles with an on-off switched drug release may offer a promising pattern to deliver a wide variety of hydrophobic payloads to tumor cells for cancer therapy.

these anticancer drugs still represent a challenge for the further study and clinical applications.³⁻⁵

Recently, pH-responsive polymers have attracted more and more attention due to their unique properties,^{6, 7} and stimuli-responsive micelles have emerged as vehicles for smart drug delivery based on the release of drugs can be readily modulated by exerting an appropriate stimulus such as temperature,⁸⁻¹⁰ pH.¹¹⁻¹³ Micelles could offer great potential and promising approach to deliver hydrophobic drugs into tumor site, which could improve the apparent water solubility and provide both passive and active targeting capabilities in order to enhance drug delivery efficacy and reduce drug side effects.^{3, 14, 15} During the circulation process in the body, drug-loaded micelles could be accumulated at the tumor cells site because of different pressure and retention effect (EPR).^{15, 16}

Moreover, inorganic/organic hybrid polymers have attracted a great deal of research interest, a particularly noticeable example is organic/inorganic hybrid polymers based on polyhedral oligomeric silsesquioxane (POSS).¹⁷⁻¹⁹ A typical POSS molecule, represented by the formula (R₈Si₈O₁₂), consists of a rigid and cubic silica core,^{20, 21} with a size in nano-scale, has also been widely investigated, since it can be introduced into polymer matrices to form hybrid polymers with thermal properties. Plenty of star-shaped polycations, POSS is

1 Introduction

In recent decades, drug delivery systems (DDSs) which are used as effective methods to treat many diseases, especially cancer therapy in order to maximize their efficacy whilst reducing toxicity.^{1, 2} However, there are still many key technical issues, such as poor solubility of the drugs, low bioavailability, side-effects, poor therapeutic effect and serious toxicities. So that, the parenteral administration application of

^aCollege of Chemistry and Chemical Engineering, Shihezi University/Key Laboratory for Chemical Materials of Xinjiang Uygur Autonomous Region/Engineering Center for Chemical Materials of Xinjiang Bingtuan, Shihezi University, Xinjiang, Shihezi 832003, China.

^bCenter for Materials Chemistry Frontier Institute of Science and Technology Xi'an Jiaotong University Xi'an, Shaanxi 710054, P. R. China.

^cState Key Laboratory of Chemical Engineering, East China University of Science and Technology, Shanghai 200237, P. R. China.

^dDepartment of immunology, Shihezi University School of Medicine/Department of Pathology and Key Laboratories for Xinjiang Endemic and Ethnic Diseases, Shihezi University School of Medicine, Xinjiang 832003, China

DOI: 10.1039/x0xx00000x

*Correspondence to: Zhiyong Liu (E-mail: zyongclin@sina.com)

†These authors contribute equally to this work.

containing a biocompatible core and display excellent performance in gene therapy. A typical POSS molecule with a three-dimensional structure of the cage consists of a cubic silica core and eight organic corner groups around outside. The eight corner organic groups can be easily modified into kinds of functional groups, such as amino, thiol, hydroxyl, and halogen^{22, 23}, POSS has been shown to improve the biocompatibility in nano-composite materials. Lastly, POSS is able to disperse the cationic charges and thus facilitating gene transfection by lowering the cytotoxicity. As a U.S. Food and drug administration approved biomedical polymer, biodegradable poly(ϵ -caprolactone) (PCL) and PCL-based biomaterials have been increasingly investigated for pharmaceutical and biomedical applications,^{7, 24} and micelles formed from block copolymers consisting of poly(ϵ -caprolactone) (PCL) and poly(ethylene glycol)methyl ether methacrylate (PEGMA) have drawn considerable interest, the PEGMA with excellent biocompatibility forms the hydrophilic corona in the micelles,^{25, 26} and in the past years, Poly(2-(N, N-dimethylamino)ethyl methacrylate) (PDMAEMA) is a weak base with a pKa at about 7. Under the pKa, PDMAEMA is hydrophilic as its amine groups are protonated. Above its pKa, PDMAEMA is hydrophobic as its amine groups are deprotonated, so PDMAEMA-based copolymers have been developed to achieve reduced toxicity and enhanced transfection activity. Doxorubicin (DOX) was selected as the model drugs.^{27, 28} As other cationic formulations, polyplexes of PDMAEMA also expose insufficient colloidal and serum stability, which restrict their applications in vivo.^{29, 30} Many well-defined hybrid polymers have been prepared using the living/controlled polymerization technique including hemitelechelic, telechelic and multitelechelic block hybrid polymers,^{18, 31, 32} and controlled/living radical polymerization (CRP),³³ such as atom transfer radical polymerization (ATRP),^{12, 34} ring-opening polymerization (ROP),³⁵ click chemistry³⁶ and reversible addition-fragmentation chain transfer polymerization (RAFT).^{18, 37} More recently, Zhang *et al.*³⁸ synthesized a series of amphiphilic pH-responsive mPEG-b-(PLA-co-PAE) block copolymers with different PLA/PAE ratios for hydrophobic drug delivery, and the low CMC values of these copolymers could markedly improve micellar stability and extend the range of applications of micelles in controlled drug delivery. Yang *et al.*³⁹ reported a series of amphiphilic 4- and 6-armed star copolymers 4/6AS-PCL-b-PDEAEMA-b-PPEGMA by the combination of ROP and ATRP for controlled delivery of hydrophobic anticancer drugs. Cheng *et al.*⁴⁰ synthesized a thermo-responsive PMEEEL-b-POCTCL diblock copolymer for controlling release of anticancer drug. Liu *et al.*⁴¹ reported a novel reducible and degradable brushed PDMAEMA derivatives with a relatively high molecular weight by ATRP and reduction-sensitive disulfide bonds were effective gene vectors with an excellent cytocompatibility.

However, the applications of micelles have been hampered because of the poor stability in vivo, the micellar disintegration in blood before reaching the tumor tissues may result in the premature release of encapsulated drugs, reduced therapeutic efficacy and undesired side effects.⁴²⁻⁴⁴ One of the effective strategies is to develop star micelles. In the past research, much efforts had been tried to prepare micelles for controlling drug release. Star polymers had attracted considerable attention in recent years due to their branched structures and unique physicochemical properties.^{45, 46} Star-

shaped polymers, a form of dendritic polymer, presented some unique properties and advantages, such as stability, morphology, drug loading level and responsiveness,⁴⁷ could be readily tuned, and a low intrinsic viscosity and crystallinity, high functionality.⁴⁸⁻⁵⁰ To the best of our knowledge, the drug delivery performance of these pH responsive star micelles was still far from satisfactory. Thus enhancing the accuracy of the response to a stimulus and the drug delivery effectiveness are imperative.

Herein, the work demonstrated a well-defined synthesis of star-shaped POSS-(PCL-P(DMAEMA-co-PEGMA))₁₆ polymer by click chemistry, ROP and ATRP of DMAEMA and PEGMA with the increasing of PCLs. Furthermore, the self-assembly behavior and pH-response of these micelles were investigated by UV-vis, DLS and TEM. Finally, the pH-sensitive behavior and triggered release of model drug in response to tumor-related pH were investigated, and meanwhile, the cellular uptake and cytotoxicity test to HeLa cells were also performed.

2. Experimental

2.1. Materials

Octavinyl POSS (OVPOSS) and 2, 2'-azobisisobutyronitrile (AIBN) were purchased from Aladdin, 1-thioglycerol (TG) was purchased from J&K Chemical, Ltd., DMAEMA and PEGMA ($M_n=500$ g/mol) (Aldrich) were passed through a column of activated basic alumina to remove the inhibitors. ϵ -CL (Sigma-Aldrich) was distilled under reduced pressure after being treated with CaH₂. Doxorubicin hydrochloride (DOX-HCl) was purchased from Beijing HuaFeng United Technology Corp. Tin 2-ethylhexanoate (Sn(Oct)₂, Aldrich) was distilled under reduced pressure. 2-Bromoisobutryl bromide (BIBB, Aldrich), *N, N, N', N, N'*-pentamethyldiethylenetriamine (PMDETA) was purchased from Sigma-aldrich, Copper (I) chloride (99.999%, Alfa Aesar) were used without further purification. HeLa cells (Institute of cells, CAS, Shanghai) were used as received, Enhanced Cell Counting Kit-8 (CCK-8, Shanghai, Beyotime Biotechnology), dulbecco's modified Eagle medium (DMEM), fetal bovine serum (FBS), pancreatic enzymes were obtained from biological industries. 4% Paraformaldehyde, 4', 6-Diamidino-2-phenylindole (DAPI) and Triton X-100 were purchased from Solarbio. Dichloromethane, methanol, triethylamine and tetrahydrofuran (THF) were dried over CaH₂ before use.

2.2. Characterization

¹H NMR data were obtained by Nuclear Magnetic Resonance Spectroscopy (NMR) using a BrukerDMX-500 NMR spectrometer with CDCl₃ as solvent. Fourier transform infrared spectroscopy (FT-IR) analysis was measured by IR-Affinity-1 Model spectrophotometer using KBr pellets. The molecular weight and molecular weight distribution of copolymers were measured by gel permeation chromatography (GPC) using a Viscotek TDA 302 gel permeation chromatograph and THF were used as eluent. X-ray photoelectron spectroscopy (XPS) was performed using an Axis Ultra spectrometer with a monochromatized Al-K α X-ray as excitation source (225 W). The transmittances of copolymers aqueous solutions at various temperatures were measured at a wavelength of 500 nm on a UV-visible spectrophotometer (UV-vis), dynamic light scattering (DLS) measurements were performed by a BECKMAN COULTER Delasa Nano C particle analyzer at a fixed angle of 165°. Before the light scattering measurements, the sample solutions were filtered three times by using Millipore

Teflon (Nylon) filters with a pore size of 0.45 μm . All measurements were repeated three times, and the average results were accepted as the final hydrodynamic diameter (D_h) and zeta potential (mV). TGA of pure OVPOSS, POSS-(PCL)₁₆, POSS-(PCL-P(DMAEMA-co-PEGMA))₁₆ were performed using a STA449F3 thermogravimeter (Netzsch, Germany) from 50°C to 700°C at a heating rate of 10°C min⁻¹ under nitrogen atmosphere. Confocal laser scanning microscopy images (Zeiss CLSM510) and fluorescence microscope (OLYMPUS U-RFL-T, Japan) were operated at the excitation wavelength of 480 nm. Samples for transmission electron microscopy (TEM) images were taken on an H-600 transmission electron microscope (Hitachi, Japan) operating at 120 kV.

2. 3 Synthesis of POSS-(PCL-P(DMAEMA-co-PEGMA))₁₆

2. 3. 1 Synthesis of the POSS-(OH)₁₆ and POSS-(PCL)₁₆

The synthesis procedure was carried out according to the reported methods.⁵¹ Multi-hydroxyl POSS-(OH)₁₆ were successfully synthesized via thiol-ene click chemistry between octavinyl POSS (OVPOSS) and 1-thioglycerol (TG) in the presence of 2, 2'-azobisisobutyronitrile (AIBN) as initiator, when the alkene/thiol molar ratio were 1:1, 1:2, 1:2.5, POSS-(OH)₁₆ were synthesized, and the crude were precipitated in diethyl ether for several times. In order to obtain POSS-(PCL)₁₆ with different hydrophobic segments, POSS-(PCL)₁₆ were synthesized by ROP with different feed ratios ϵ -CL using Sn(Oct)₂ as catalyst. As an example the typical procedure was as follows: POSS-(OH)₁₆ (0.5 g, 0.67 mmol), ϵ -CL (12 g, 85 mmol), Sn(Oct)₂ (0.04 g, 0.1 mmol), and anhydrous toluene (50 mL) were added into a fresh flamed and nitrogen purged round-bottomed flask and the flask was then placed in a thermostatted oil bath at 120°C for 24 h. After the polymerization, the mixture was cooled to room temperature, then, the product dissolved in dichloromethane, and precipitated three times in methanol. Finally, the precipitate was collected and dried under vacuum to a constant weight at 35°C. The different degree of polymerization (DP) of PCL were synthesised by ROP in the same way, which were named P1 and P2.

2. 3. 2 Synthesis of POSS-(PCL)₁₆-Br initiator

Typically, POSS-(PCL)₁₆ (4 g, 0.2mmol) and triethylamine (3 mL) were first added into a 100 mL dry flask and 30 mL of anhydrous CH₂Cl₂ was added to dissolve POSS-(PCL)₁₆ under nitrogen atmosphere, then the flask was placed in an ice/water bath. 3.0 mL of 2-bromoisobutryl bromide was added dropwise into the flask over 1 h, and the reaction mixture was stirred 48 h at 30°C. The precipitate was filtered off. Then, the filtrate was washed three times sequentially with an aqueous solution of sodium bicarbonate and water. The product was further concentrated by a rotary evaporator, and precipitated three times in methanol, and dried under vacuum to a constant weight at 35°C.

2. 3. 3 Synthesis of POSS-(PCL-P(DMAEMA-co-PEGMA))₁₆ by ATRP

Synthesis of POSS-(PCL-P(DMAEMA-co-PEGMA))₁₆: a series of POSS-(PCL-P(DMAEMA-co-PEGMA))₁₆ were prepared by ATRP of DMAEMA and PEGMA using POSS-(PCL)₁₆-Br as initiator and CuBr/PMDETA as catalyst with different hydrophobic cores, the reaction procedures were shown in Scheme 1, and named PD1, PD2.

For example, star-shaped inorganic/organic hybrid copolymers POSS-(PCL-P(DMAEMA-co-PEGMA))₁₆ by ATRP of DMAEMA and PEGMA with multifunctional POSS-(PCL)₁₆-Br as initiator was described below. POSS-(PCL)₁₆-Br (0.5 g, 0.03 mmol), DMAEMA (2.8 g, 9.0 mmol), PEGMA (2.2 g, 1.0 mmol), CuBr (0.151 g, 1.0 mmol), PMDETA (0.337 g, 2 mmol), and THF (30 mL). The flask was degassed with three freeze-evacuate-thaw cycles. Then, the polymerization was performed at 65°C for 12 h. After being cooled to room temperature, the reaction flask was open to air, and the crude product was diluted with THF and passed through a neutral alumina column to remove the copper catalysts. Finally it was precipitated thrice into cold hexane, and dried under vacuum to a constant weight at 40°C.

2. 4 Self-assembly of POSS-(PCL-P(DMAEMA-co-PEGMA))₁₆ in aqueous solution

Samples for UV-vis, DLS and TEM were prepared as follows: PD1 and PD2 (20 mg) were dissolved in THF (2 mL) and subsequently, deionized water (1 mL) were added dropwise from an additional funnel over a period of 30 min. After 4 h quick stirring, 8 mL water was added to quench the micellar assembly, subsequently dialyzed (molecular weight cut-off: 7000 Da) against with distilled water for 72 h. During this dialysis process, the hybridized copolymers self-assembled into micelles with POSS, PCL cores and star-shaped P(DMAEMA-co-PEGMA) coronas. Polymeric micelles with different concentrations could be obtained by diluting with distilled water and equilibrating at room temperature for 48 h.

2. 5 DOX encapsulation and release studies

100 mg of PD1/PD2 and 10 mg of DOX•HCl were dissolved in 4 mL of DMF separately and the two solutions were mixed in a vial and stirred for 30 min, a 3-fold excess of TEA in 4 mL DMF overnight to obtain DOX base. Then the mixture were added dropwise using a syringe pump to water (80 mL). The DOX-containing suspension were then equilibrated under stirring at room temperature for 4 h, followed by thorough dialysis (molecular weight cut-off: 3500 Da) against deionized water for 2 days to remove unloaded DOX, which were named D-PD1 and D-PD2.

The DOX loading content (DLC) and loading efficiency (DLE) were determined by UV-vis spectrophotometry at 480 nm. To determine the drug loading level, a small portion of DOX-loaded micelles was withdrawn and diluted with DMF to a volume ratio of DMF/H₂O=9/1. The amount of DOX encapsulated were quantitatively determined by a UV-vis spectrophotometer and the calibration curve used for drug loading characterization were established by the intensity of DOX with different concentrations in DMF/H₂O=9/1 (v/v) solutions. The DLC were defined as the weight ratio of entrapped DOX to that of the DOX-loaded micelles. The DLE of DOX was obtained as the weight ratio between DOX incorporated in assembled micelles and that used in fabrication.

$$\text{DLC}(\text{wt}\%) = \frac{\text{weight of loaded drug}}{\text{weight of polymer}} \times 100 \quad (1)$$

$$\text{DLE}(\text{wt}\%) = \frac{\text{weight of loaded drug}}{\text{weight of drug in feed}} \times 100 \quad (2)$$

The in vitro DOX release profiles from the PD1/PD2 assembled micelles were evaluated using buffers solution with pH values 5.0 and 7.4, then placed in a dialysis bag (molecular weight cut-off: 3500). The whole bag was placed into 35 mL PBS or acetate buffer and shaken (200 rpm.) at 37°C.

At specified time intervals 4 mL (V_e) samples were taken and an equal volume of fresh buffer added to maintain the total volume. The concentration of DOX in different samples was analyzed by UV-vis spectrophotometry at 480 nm. The cumulative percent drug release (E_r) was calculated using E_q , (1).

$$E_r(\%) = \frac{V_e \sum_{i=1}^{n-1} C_i + V_e C_n}{m_{DOX}} \times 100 \quad (3)$$

Where m_{DOX} represented the amount of DOX in the micelle, V_e was the volume of the release medium ($V_e = 70$ mL), C_i represented the concentration of DOX in the i th sample and C_n represented the concentration of DOX in the n th sample. The in vitro release experiments were carried out in triplicate at each pH and the reported results were the average values with standard deviations.

2. 6 Cytotoxicity test

The cytotoxic effects of polymers, free DOX and DOX-loaded POSS-(PCL-P(DMAEMA-co-PEGMA))₁₆ micelles were evaluated against HeLa cells by the standard XTT. To perform cytotoxicity assay, HeLa cells were seeded at a density of 5000 cells per well on a 96-well plate and cultured for 24 h. The samples were prepared at a series of desired concentrations. Every experimental well was treated with the samples for 24 h and others were added with fresh medium as control. After 24 h incubation, CCK-8 was added into each well to dissolve the formazan by pipetting in and out several times. The absorbance of each well was measured at a test wavelength of 450 nm. The cell viability of samples were calculated as follow: 5, 52, 53

$$\text{Cell viability}(\%) = \frac{A_{\text{test}} - A_{\text{blank}}}{A_{\text{control}} - A_{\text{blank}}} \times 100 \quad (4)$$

Where A_{test} and A_{control} represent the intensity determined for cells treated with different samples and for control cells, respectively, and A_{blank} is the absorbance of wells without cells.

2. 7. Intracellular release of DOX

Confocal laser scanning microscopy (CLSM) was used to visualize the subcellular localization and intracellular release behavior of DOX-loaded micelles and free DOX for various lengths of time (0.5 h, 4 h and 24 h). First, the HeLa cells were seeded in a glass base dish with a coverslip at a density of 5000 cells and cultured in DMEM supplemented with 10% FBS for 24 h. Then DOX-loaded micelles and free DOX was added, and cells were cultured for 0.5 h, 4 h and 24 h in a humidified 5% CO₂-containing atmosphere. Finally, the location of intracellular fluorescence was validated using a CLSM imaging system (Zeiss CLSM510) at the excitation wavelength of 480 nm.

3. Results and discussion

3. 1. Characterization of POSS-(OH)₁₆, POSS-(PCL)₁₆ and POSS-(PCL-P(DMAEMA-co-PEGMA))₁₆: FT-IR analysis result of POSS-(OH)₁₆, POSS-(PCL)₁₆ and POSS-(PCL-P(DMAEMA-co-PEGMA))₁₆ copolymers were shown in Fig 1. The absorption at 1750 cm⁻¹ could be ascribed to the characteristic carbonyl (C=O) stretching vibration of PCL and PDMAEMA (Fig. 1(b) and 1(c)), we could not find the characteristic carbonyl (C=O) stretching vibration in Fig. 1(a). The characteristic peaks of PDMAEMA were as follows: 2770 and 2821 cm⁻¹ from C-H stretching vibration in the -N(CH₃)₂ group (Fig. 1(c)). The absorption at 3437 cm⁻¹ could be ascribed to the characteristic hydroxyl (O-H) stretching vibration of POSS-(OH)₁₆, POSS-(PCL)₁₆ and POSS-(PCL-P(DMAEMA-co-PEGMA))₁₆ in Fig. 1. It demonstrated POSS-(PCL)₁₆ and POSS-(PCL-P(DMAEMA-co-PEGMA))₁₆ polymerization successfully. POSS-(OH)₁₆ with different ratios of OVPOSS and TG were prepared by changing the feed ratios of the thiol and alkene, the ¹H NMR spectra of OVPOSS/TG molar ratios (1:1, 1:2, 1:2.5) were shown in Fig. 2, the chemical shifts in Fig. 2(a), (b) and (c) at 0.993 ppm, 1.760 ppm, 2.502 ppm, 3.558 ppm were attributed to the proton signals of methylene groups in POSS-(OH)₁₆, and at 4.542 ppm and 4.721 ppm were attributed to the proton signals of hydroxyl in TG. However, when the alkene/thiol molar ratios were 1:1, 1:2, the signals of resonance at 5.972 ppm, 6.156 ppm were assignable to the protons from the vinyl group of OVPOSS units, when the alkene/thiol molar ratio were 1:2.5, the signals at 5.972 ppm and 6.156 ppm of vinyl group of OVPOSS units disappeared completely, which further confirmed the formation of POSS-(OH)₁₆ completely. The structural characteristics of the obtained star-shaped POSS-(PCL)₁₆ and POSS-(PCL-P(DMAEMA-co-PEGMA))₁₆ have been determined by ¹H NMR analysis in Fig. 3 and Fig. 4 the resonance at 4.077 ppm (a), 2.323 ppm (b), 1.670 ppm (c), and 1.394 ppm (d) were the characteristic signal of the methylene protons at different positions of PCL group respectively, in the upper diagram POSS-(PCL-P(DMAEMA-co-PEGMA))₁₆ some new peaks from (DMAEMA and PEGMA)_n units could be seen in Fig. 4, the signals at 4.180 ppm (f) and 0.0903 (d) were ascribed to -CH₂OCO and -CCH₂C- of the DMAEMA and PEGMA units, respectively. The signals at 1.409 ppm (e), 1.943 ppm (i), 2.590 ppm (h), 1.062 ppm (a) were ascribed to -CH₂CCH₃, -CH₂CCH₃, -CH₂NCH₃ and -CH₂NCH₃ of the DMAEMA units, the signals at 1.860 ppm (c), 3.663 ppm (g), 3.388 ppm (b) were ascribed to -CH₂CCH₃, -CH₂CH₂O- and -CH₂OCH₃ of the PEGMA units, it were confirmed that the block copolymer had been produced. As shown in Fig. 3, the peaks of the protons in POSS-(PCL)₁₆ were overlapped by the signals of protons in P(DMAEMA-co-PEGMA). Therefore, it was difficult to calculate the molecular weight of the copolymers according to ¹H NMR spectrum.

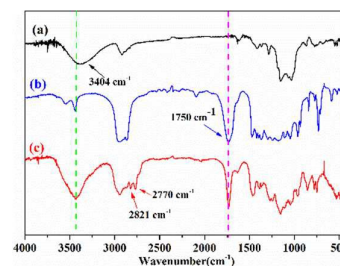
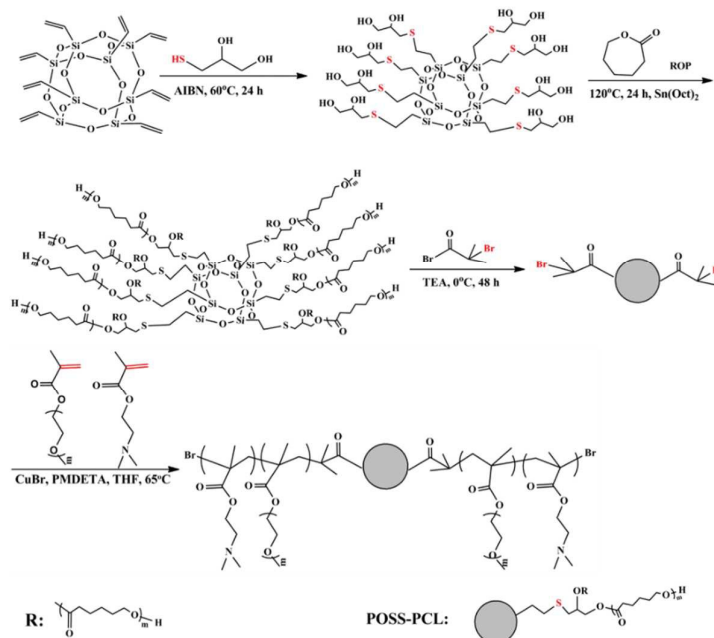


Fig. 1 FT-IR spectra of POSS-(OH)₁₆ (a), POSS-(PCL)₁₆ (b) and POSS-(PCL-P(DMAEMA-co-PEGMA))₁₆ (c).



Scheme 1. Synthesis of pH-responsive star-shaped POSS-(PCL-P(DMAEMA-co-PEGMA))₁₆ inorganic/organic hybrid block copolymers

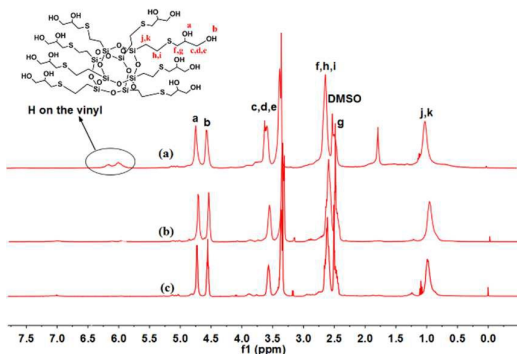


Fig. 2 The ¹H NMR spectra of POSS-(OH)₁₆ (a) the alkene/thiol molar ratio were 1:1, (b) 1:2, (c) 1:2.5.

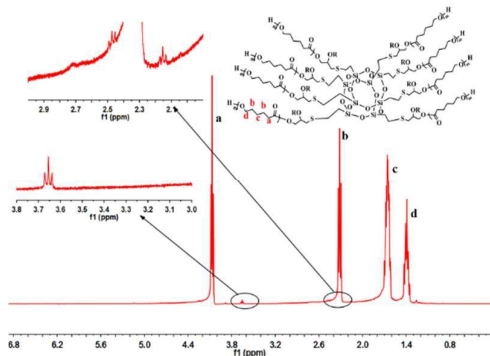


Fig. 3 The ¹H NMR spectrum of POSS-(PCL)₁₆.

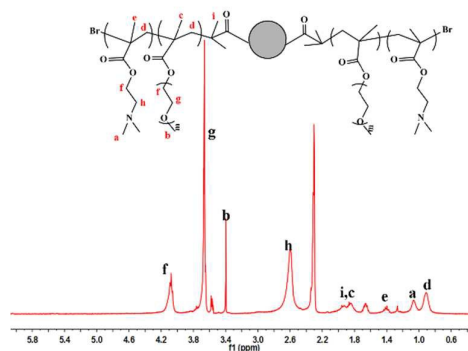


Fig. 4 The ¹H NMR spectrum of POSS-(PCL-P(DMAEMA-co-PEGMA))₁₆ block copolymer.

Table 1 Characterization of POSS-(PCL-P(DMAEMA-co-PEGMA))₁₆ copolymers

Samples ^a	M_n , Th ^b	M_n , GPC ^c	M_w/M_n ^c
P1	38017	33741	1.45
PD1	78016	74021	1.15
P2	69025	61083	1.48
PD2	117950	133081	1.06

^aP1 represent the short PCL segments; and P2 represent the long PCL segments; ^bCalculated by theory analysis from the feed ratio of monomers to initiator; ^cPolymerization conditions [monomer]₀/[POSS-(PCL)₁₆]

$Br]_0/[CuBr]_0/[PMDETA]_0=100/1/1/2$, measured by GPC calibrated with PS standards. THF was used as eluent.

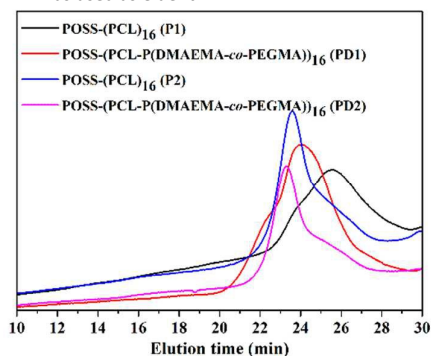


Fig. 5 Evolution of GPC chromatograms of POSS-(PCL)₁₆ (P1 and P2) and POSS-(PCL-P(DMAEMA-co-PEGMA))₁₆ (PD1 and PD2) block copolymers with different molecular weights.

As we seen in Fig 5, the GPC traces of POSS-(PCL-P(DMAEMA-co-PEGMA))₁₆ block copolymers were shown in Fig. 5. All the curves of POSS-(PCL-P(DMAEMA-co-PEGMA))₁₆ (PD1 and PD2) shifted to lower elution volume compared to that of POSS-(PCL)₁₆ (P1 and P2). The polymerization results were also listed in Table 1. The GPC results were almost consistent with the theoretical values, suggesting that well-defined POSS-(PCL-P(DMAEMA-co-PEGMA))₁₆ block copolymers were synthesized and characterized successfully.

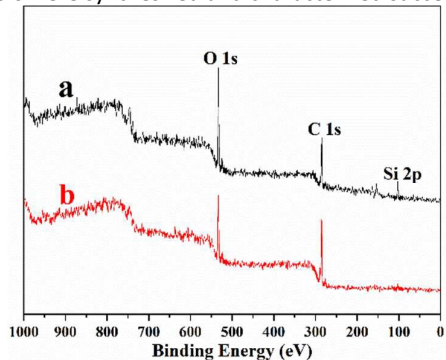


Fig. 6 XPS survey spectra of POSS-(OH)₁₆ (a) and POSS-(PCL-P(DMAEMA-co-PEGMA))₁₆ (b) (PD1).

XPS analysis also verified the composition of POSS-(OH)₁₆ and POSS-(PCL-P(DMAEMA-co-PEGMA))₁₆. Fig. 6 showed the full scan spectra of POSS-(OH)₁₆ and POSS-(PCL-P(DMAEMA-co-PEGMA))₁₆, revealing the peaks corresponding to carbon, oxygen, and silicon atoms at characteristic binding energies. Meanwhile, the element contents of C, O, and Si were 57.75, 31.11, and 11.14% in POSS-(OH)₁₆, respectively. For POSS-(PCL-P(DMAEMA-co-PEGMA))₁₆, the element contents of C, O and Si changed to 74.38, 24.31, and 1.31%, respectively (Table 2).

Table 2. Element content of POSS-(OH)₁₆ and POSS-(PCL-P(DMAEMA-co-PEGMA))₁₆s

Element content	POSS-(OH) ₁₆	PD1
C%	57.75	74.38
O%	31.11	24.31
Si%	11.14	1.31

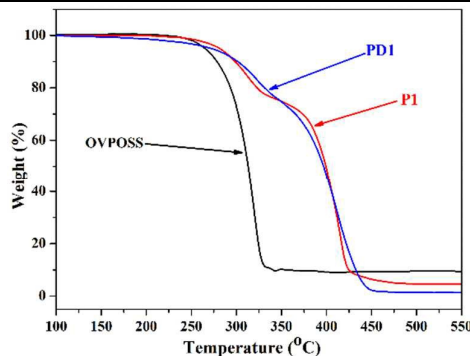


Fig. 7 TG curves of OVPOSS, POSS-(PCL)₁₆ (P1) and POSS-(PCL-P(DMAEMA-co-PEGMA))₁₆ (PD1).

As seen in Fig 7, thermogravimetric analysis was used in an investigation of the decomposition pattern and the thermal stability of three kinds of polymers. The thermal decomposition of OVPOSS homopolymer occurred by a one-step mechanism started at 264°C and completed at about 359°C. And the thermal decomposition of POSS-(PCL)₁₆ and POSS-(PCL-P(DMAEMA-co-PEGMA))₁₆ started at 282°C and 273°C. It indicated the thermal stability of triblock polymers were superior to OVPOSS, which indicated that the thermal property of copolymers could improve successfully.

3. 2 Formation and characterization of the blank and DOX-loaded star-shaped D-PD1 and D-PD2 micelles

As shown in Scheme 2(A), as an amphiphilic block copolymers, when the concentration were above the critical micelle concentration (CMC), POSS-(PCL-P(DMAEMA-co-PEGMA))₁₆ could self-assemble into micelles in selective solvent. The hydrophilic P(DMAEMA-co-PEGMA) arm chains were mainly in the corona of the micelles, whereas the hydrophobic POSS and PCL side chains in the star-shaped copolymer were mainly in the core of the micelles. The hydrophobic of POSS and PCL as cores have been extensively used for drug delivery system because of the larger cores, which were named PD1 and PD2 micelles. DOX was physically incorporated into PD1 and PD2 copolymer micelles, which were named D-PD1 and D-PD2. The physico-chemical properties of the blank and DOX-loaded micelles were characterized by DLS analysis. The average particle sizes, polydispersity index (PDI), zeta potentials of the blank and DOX-loaded micelles were summarized in Table 3.

Table 3 Hydrodynamic diameter (D_h), size distributions (PDI) and Zeta potentials of blank and DOX-loaded POSS-(PCL-P(DMAEMA-co-PEGMA))₁₆ micelles.

Micelle	Blank			DOX-load				
	D_h (nm)	PDI	Zeta (mV)	D_h (nm)	PDI	Zeta (mV)	DLC (wt%)	DLE (wt%)
PD1	215.±1.5	0.213±0.018	14.43±0.22	294.4±3.5	0.23±0.023	5.4±0.012	6.05	60.5
PD2	281.4±2.7	0.197±0.007	16.68±0.34	383.1±2.8	0.06±0.007	8.25±0.25	7.56	75.6

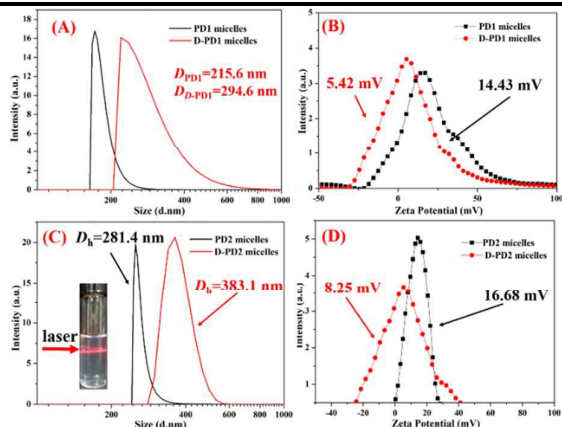
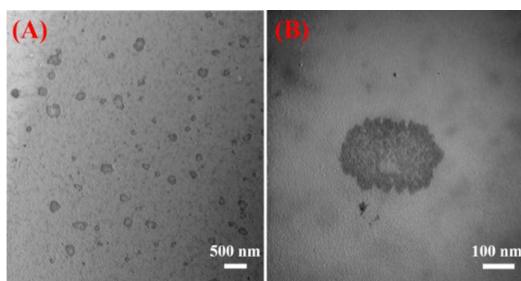
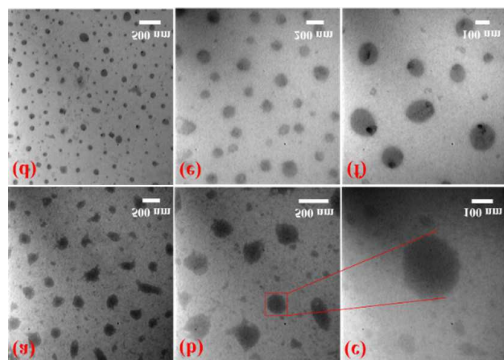
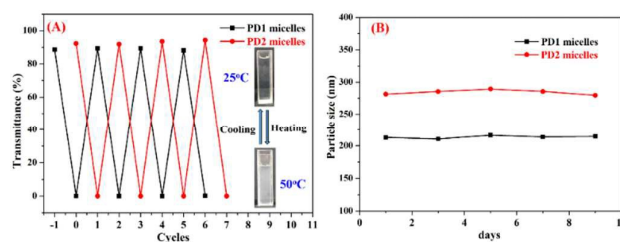


Fig. 8 The particle size distribution curves corresponding to the samples in (A), (C) and zeta potentials of DOX-loaded micelles in (B), (D) (PD1, D-PD1, PD2 and D-PD2).

Fig. 9 TEM images of DOX-loaded POSS-(PCL-P(DMAEMA-co-PEGMA))₁₆ micelles (PD2 (A, B)).Fig. 10 TEM images of POSS-(PCL-P(DMAEMA-co-PEGMA))₁₆ micelles (PD1 (a, b, c) and PD2 (d, e, f)).Fig. 11 Plots of transmittance as a function of temperature for POSS-(PCL-P(DMAEMA-co-PEGMA))₁₆ micelle (A), particle size of the PD1 and PD2 micelles at room temperature (B).

As shown in Fig. 8, The hydrodynamic diameter, polydispersity index (PDI) and zeta potential of the POSS-(PCL-P(DMAEMA-co-PEGMA))₁₆ micelles were evaluated by DLS and TEM. The combination of TEM and DLS confirmed that the spherical star shaped polymeric assemblies loaded with DOX. Compared with blank micelles, The D-PD micelles presented a nanoscaled particle size with a narrow particle size distribution, a low zeta potential with a positive surface charge due to the tertiaryamine groups in the PDEAEMA segments (Fig. 8, Fig. 9, Table 3), when DOX was loaded into micelles in the core and adsorbed drug on the surface. It could also be found that the zeta potentials of the drug-loaded micelles were slightly lower than those of blank micelles for both of the polymers, resulting from decreased charge density because of larger particle sizes in the Table 3. TEM micrographs showed that the micelles and D-PD1 have a nearly spherical morphology, as shown in Fig. 9 and 10, which displayed the TEM images of the polymeric micelles with PD1 and PD2 and showed that the dried micelles dispersed as discrete spots, the sizes of the micelles determined by TEM were about 150 nm and 200 nm for PD1 and PD2. Compared with the determination by DLS, the shrinkage of the micellar shell during the TEM samples preparation process may have led to a decrease in the size of the micelles. Moreover, the TEM images showed a broader distribution of particle size compared with the DLS data, this discrepancy could be ascribed to the fact that TEM were a qualitative method and only showed a localized viewing field. As shown in Fig. 11, a stability assay in terms of transmittance and particle size of the PD1 and PD2 micelles were investigated in water for (A) and (B), the PD1 and PD2 micelles presented reversible transformation of transparency and turbidity during the reversible cooling and heating cycles in Fig. 11(A), obviously, the phase transition of micelles were reversible, which indicated that the PD1 and PD2 micelles were stable. As shown in

Fig. 11(B), no obvious change of the particle size of the PD1 and PD2 micelles in water during 9 days indicated that the micelles had a well long-term stability without the presence of precipitation and phase separation. The result revealed that the PD1 and PD2 could offer the protection of drugs from untimely structure disintegration and premature drug release until arriving a disease site.

3. 3 In vitro release of DOX from micelles

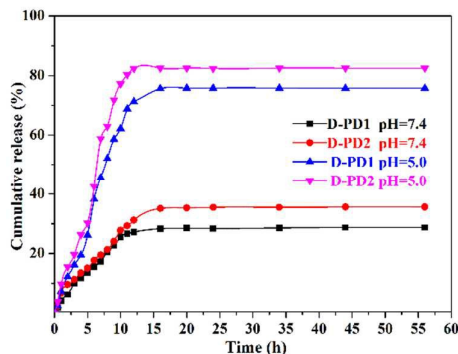


Fig. 12 In vitro release of DOX from various DOX-loaded micelles at 37°C under different pH conditions.

As expected, the POSS-(PCL-P(DMAEMA-co-PEGMA)₁₆) micelles exhibited a pH-responsive characteristic. In vitro drug release performances of the micelles were performed under physiological conditions (PBS, pH 5.0 and 7.4) at 37°C as shown in Fig. 12. It could be observed that the drug release rates of DOX from the particles were obviously changed by pH values as well as time. With regard to pH of 7.4 at 37°C, the micelles stayed compact and the loaded DOX was released slowly. After 3 h, less than 20% of DOX (11% and 13% for D-PD1 and D-PD2, respectively) were released. Even after 24 h, only about 30% and 33% for D-PD1 and D-PD2, respectively. In contrast, when the pH was lower at 37°C (pH 5.0), the drug release were accelerated, after 24 h, the cumulative release were 78% and 82% for D-PD1 and D-PD2 micelles, respectively. The result were due to the swollen drug-loaded micelles, attributing to the protonation of amino groups in PDEAEMA segments at acidic conditions, the micelles started to associate due to the protonation of P(DMAEMA-co-PEGMA) corona. Herein, the copolymers with specific random pH-sensitive/hydrophilic/hydrophobic structure could satisfy the requirements of fast, short-time and efficient drug release for special occasions. Meanwhile, the DOX molecules were not only encapsulated inside the micellar core, but also absorbed by the P(DMAEMA-co-PEGMA) shell due to the electric action, while only that loaded by hydrophobic effect could be released comparative fast, so it may spend extended period to achieve complete release. As may be concluded from the discussion above, these PD1 and PD2 micelles were just like on-off switching nanocarriers in release kinetics by changing pH values. Therefore, it was highly interesting for intracellular anti-cancer drug delivery.

3. 4 Cytotoxicity test

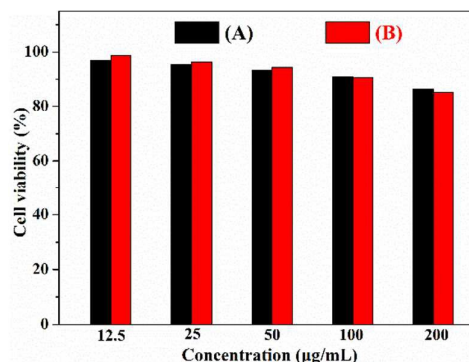


Fig. 13 In vitro cell viability of the PD1 and PD2 micelles. Concentration-dependent cell viability of HeLa cells treated with the PD1 (A) and PD2 (B) after incubation of 48 h.

Cytotoxic effects of the polymers, free DOX or DOX-loaded micelles in HeLa cells were determined by CCK-8 assay. The cell viability of POSS-(PCL-P(DMAEMA-co-PEGMA)₁₆) based blank micelles and DOX-loaded micelles against HeLa cells were evaluated. The cell viability of blank micelles was measured after 48 h incubation. As shown in Fig 13, the blank micelles with different concentration were nontoxic to HeLa cells and the cell viability were over 90% at all concentrations (12.5~200 µg/mL). This indicated that all POSS-(PCL-P(DMAEMA-co-PEGMA)₁₆) polymeric micelles were nontoxic and biocompatible and could be used as a delivery system for anticancer agents.

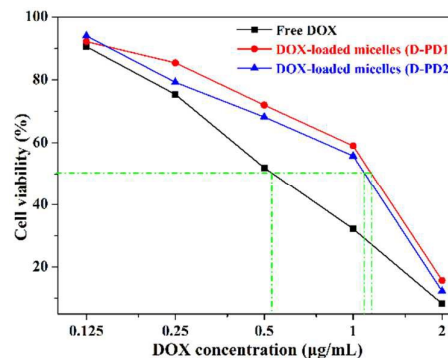


Fig. 14 Cell viability of HeLa cells incubated with free DOX and DOX-loaded micelles (D-PD1 and D-PD2) for 48 h at different concentrations.

As we shown in Fig. 14, it showed the results of samples treated with free DOX or DOX-loaded micelles for 48 h, respectively. The DOX dosages required for the inhibitory concentration to produce 50% cell death (IC₅₀) were 0.551 µg/mL, 1.208 µg/mL, 1.133 µg/mL for 48 h for free DOX, D-PD1 and D-PD2 against HeLa cells. This slight difference between two DOX-loaded micelles could be explained that the latter containing more pH-sensitive PDEAEMA units, leading to higher drug loading level and more sensitive respectively. All of DOX-loaded micelles had a similar capacity of killing tumor cells as free DOX for 48 h, indicating that DOX enveloped by micelles might not inhibit the ability of DOX killing the cells although slowed down the release of DOX, and both of the DOX loaded micelles showed slightly lower cytotoxicity than free DOX due to the time-consuming DOX release from DOX loaded micelles at the same DOX concentration. The result revealed that

DOX released from the micelles could exploit a potent drug efficacy as free DOX after entry into the HeLa cells, produce the desired pharmacological action and minimize the side effect of free DOX.

3. 5 In vitro cellular uptake studies

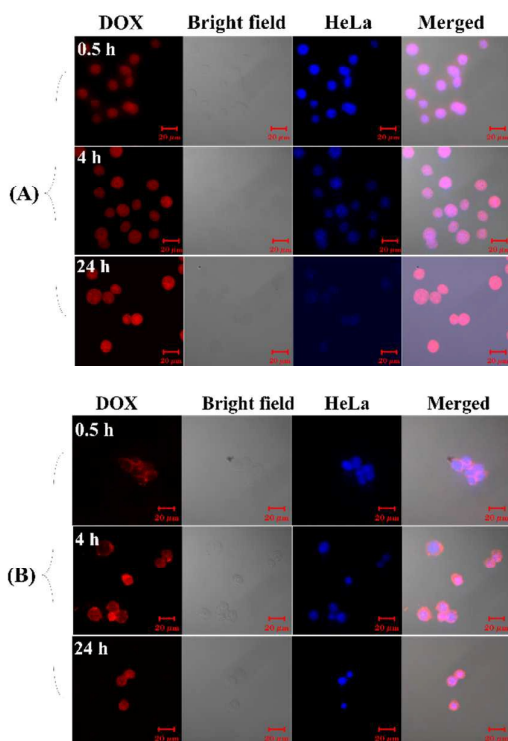


Fig. 15 Confocal laser scanning microscopy images of HeLa cells incubated with (A) free DOX and (B) DOX-loaded (D-PD2) for different times. The DOX dosage was 10 $\mu\text{g}/\text{mL}$. For each panel, images from left to right show cell nuclei stained by DOX fluorescence in cells (red), bright field of cells, HeLa (blue), and overlays of the blue and red images. The scale bars are 20 μm in all images.

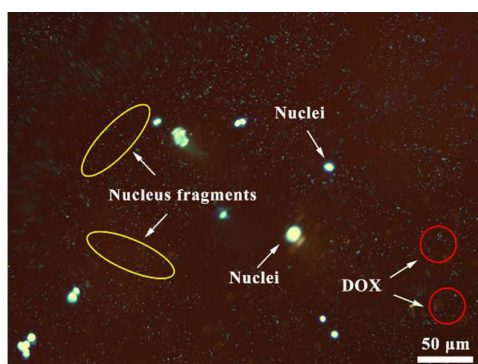
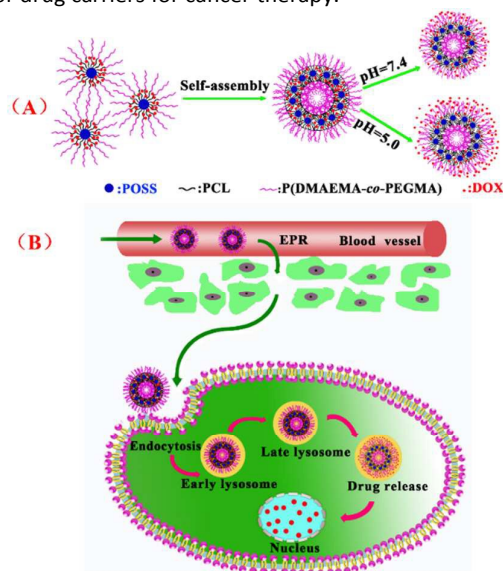


Fig. 16 Fluorescence images of HeLa cells incubated with DOX-loaded (D-PD2) for 24 h. DOX fluorescence in cells (red), bright field of cells, HeLa (blue), and overlays of the blue and red images. The scale bars are 50 μm in all images.

To evaluate the intracellular uptake efficiency, CLSM were used to identify the location of the DOX in HeLa cells. The

confocal laser scanning microscopy images of HeLa cells after 0.5 h, 4 h and 24 h of incubation with free DOX and D-PD2 were presented in Fig. 15. After incubation for 0.5 h, stained with DAPI, the nuclei and cytoplasm of pretreated cells were observed by CLSM. By comparison with the control in Fig. 15(B), the observation revealed that free DOX was slightly accumulated in the cell nuclei of HeLa cells in Fig. 15(A). After incubation for 4 h and 24 h, free DOX was larger accumulated than D-PD2, and while DOX released from DOX loaded micelles (D-PD2) was mainly located in the cytoplasm, and DOX was released into the cytoplasm and nuclei of cells under acid conditions in lysosomes in Fig. 15(A and B), the schematic illustration of this pH-responsive degradation process and the efficient intracellular release of anti-cancer drugs could be explained by Scheme 2. After 24 h of incubation with DOX-loaded micelles (D-PD2), it indicated the nuclei of HeLa cells were dissociated by DOX-loaded micelles (D-PD2) in Fig. 16, which exhibited a higher inhibition of the proliferation of HeLa cells. Moreover, the result also indicated that free DOX was taken up by diffusion through the cell membrane and the DOX loaded micelles were taken up by the nuclei of cells via the endocytosis process. Moreover, the self-assembled micelles of the amphiphilic copolymer show a great potential as anti-tumor drug carriers for cancer therapy.



Scheme 2. Illustration of pH-responsive self-assembly of the amphiphilic copolymer of POSS-(PCL-P(DMAEMA-co-PEGMA))₁₆ for the efficient intracellular release of anti-cancer drugs triggered by the acidic microenvironment inside the tumor tissue.

4. Conclusion

In the current work, we have designed and synthesized pH-responsive star-shaped POSS-(PCL-P(DMAEMA-co-PEGMA))₁₆ copolymers with different PCL segments by click chemistry, ROP and ATRP. These polymers could self-assemble into micelles comprising of POSS and PCL cores and P(DMAEMA-co-PEGMA) shells in aqueous solution. The hydrodynamic diameter, polydispersity index (PDI) and zeta potential of the POSS-(PCL-P(DMAEMA-co-PEGMA))₁₆ polymeric micelles were evaluated by DLS and TEM, the sizes of the micelles determined by TEM were about 150 nm and 200 nm with spherical shapes for PD1 and PD2.

The particle size and reversible transformation of transparency and turbidity were enhanced stability and prolonged cycle length by DLS and UV-vis, these copolymers could markedly improve micellar stability and extend the range of applications of micelles in controlled drug delivery with increasing PCL segments.

The in vitro release behaviors of DOX from PD1 and PD2 micelles exhibited pH-responsive. The DOX loading contents were higher as the PCL segments increased. The release of DOX from the micelles were significantly accelerated by decreasing pH from 7.4 to 5.0 at 37°C, and after 55 h for DOX-loaded micelles, the cumulative release was about 82% (w/w), which could be provided sustained drug delivery behavior after the DOX-loaded micelles entered into blood circulation by endocytosis. The blank copolymer micelles revealed bare toxicity for the HeLa cells. The DOX-loaded polymeric micelles showed much higher toxic effect for the HeLa cells, which was almost similar to free DOX. And the DOX-loaded micelles were taken up by the nuclei of cells via the endocytosis process by CLSM, which exhibited inhibition of the proliferation of HeLa cells. Furthermore, the applicability of these micelles in response to cellular components toward tumor-targeting delivery applications in vivo is an exploratory research area.

Acknowledgements

The authors gratefully acknowledge financial supports from the National Natural Science Foundation of China (21367022) and Bingtuan Innovation Team in Key Areas (2015BD003).

References

- [1] R. Negrini, W.-K. Fong, B.J. Boyd, R. Mezzenga, *Chem Commun.*, 2015, **51**, 6671-6674.
- [2] C.Y. Zhang, W.S. Wu, N. Yao, B. Zhao, L.J. Zhang, *RSC Adv.*, 2014, **4**, 40232-40240.
- [3] Y.Q. Yang, X.D. Guo, W.J. Lin, L.J. Zhang, C.Y. Zhang, Y. Qian, *Soft Matter*, 2012, **8**, 454-464.
- [4] W. She, N. Li, K. Luo, C. Guo, G. Wang, Y. Geng, Z. Gu, *Biomaterials.*, 2013, **34**, 2252-2264.
- [5] C. Yu, C. Gao, S. Lü, C. Chen, J. Yang, X. Di, M. Liu, *Colloid Surface B.*, 2014, **115**, 331-339.
- [6] J. Chen, M. Liu, C. Gao, S. Lü, X. Zhang, Z. Liu, *RSC Adv.*, 2013, **3**, 15085-15093.
- [7] J. Chen, M. Liu, H. Gong, Y. Huang, C. Chen, *J Phys Chem B.*, 2011, **115**, 14947-14955.
- [8] X. Huang, Y. Xiao, M. Lang, *J Colloid Interf Sci.*, 2011, **364**, 92-99.
- [9] V. Ladmiral, M. Semsarilar, I. Canton, S.P. Armes, *J Am Chem Soc.*, 2013, **135**, 13574-13581.
- [10] R. Paris, I. Quijada-Garrido, *Eur Polym J.*, 2010, **46**, 2156-2163.
- [11] B. Sahoo, K.S. Devi, R. Banerjee, T.K. Maiti, P. Pramanik, D. Dhara, *ACS Appl Mater Inter.*, 2013, **5**, 3884-3893.
- [12] J. Mao, X. Ji, S. Bo, *Macromol Chem Phys.*, 2011, **212**, 744-752.
- [13] M. Siauw, P.A. FitzGerald, B.S. Hawkett, S. Perrier, *Soft Matter*, 2013, **9**, 7007-7015.
- [14] J. Ding, C. Xiao, Y. Li, Y. Cheng, N. Wang, C. He, X. Zhuang, X. Zhu, X. Chen, *J Control Release.*, 2013, **169**, 193-203.
- [15] C.Y. Zhang, W.S. Wu, N. Yao, B. Zhao, L.J. Zhang, *RSC Adv.*, 2014, **4**, 40232-40240.
- [16] H. Hussain, K.Y. Mya, C. He, *Langmuir*, 2008, **24**, 13279-13286.
- [17] C. Sanchez, P. Belleville, M. Popall, L. Nicole, *Chem Soc Rev.*, 2011, **40**, 696-753.
- [18] L. Hong, Z. Zhang, W. Zhang, *Ind Eng Chem Res.*, 2014, **53**, 10673-10680.
- [19] A. Franczyk, H. He, J. Burdyńska, C.M. Hui, K. Matyjaszewski, B. Marciniak, *ACS Macro Lett.*, 2014, **3**, 799-802.
- [20] X. Wang, S. Xuan, L. Song, H. Yang, H. Lu, Y. Hu, *J Macromol Sci B.*, 2012, **51**, 255-268.
- [21] M.J. Fernández, M.D. Fernández, M. Cobos, *RSC Adv.*, 2014, **4**, 21435-21449.
- [22] S.-W. Kuo, F.-C. Chang, *Prog Polym Sci.*, 2011, **36**, 1649-1696.
- [23] S. Yilmaz, M. Kodal, T. Yilmaz, G. Ozkoc, *Compos Part B-Eng.*, 2014, **56**, 527-535.
- [24] P. Sun, Y. Zhang, L. Shi, Z. Gan, *Macromol Biosci.*, 2010, **10**, 621-631.
- [25] S. Shahalom, T. Tong, S. Emmett, B.R. Saunders, *Langmuir*, 2006, **22**, 8311-8317.
- [26] J.-F. Lutz, A. Hoth, *Macromolecules*, 2006, **39**, 893-896.
- [27] C. Zhu, M. Zheng, F. Meng, F.M. Mickler, N. Ruthardt, X. Zhu, Z. Zhong, *Biomacromolecules*, 2012, **13**, 769-778.
- [28] K.H. Min, J.-H. Kim, S.M. Bae, H. Shin, M.S. Kim, S. Park, H. Lee, R.-W. Park, I.-S. Kim, K. Kim, *J Control Release.*, 2010, **144**, 259-266.
- [29] G. Liu, S. Ma, S. Li, R. Cheng, F. Meng, H. Liu, Z. Zhong, *Biomaterials*, 2010, **31**, 7575-7585.
- [30] S. Guo, Y. Huang, T. Wei, W. Zhang, W. Wang, D. Lin, X. Zhang, A. Kumar, Q. Du, J. Xing, *Biomaterials*, 2011, **32**, 879-889.
- [31] B.H. Tan, H. Hussain, C.B. He, *Macromolecules*, 2011, **44**, 622-631.
- [32] Y.S. Ye, W.C. Shen, C.Y. Tseng, J. Rick, Y.J. Huang, F.C. Chang, B.J. Hwang, *Chem Commun.*, 2011, **47**, 10656-10658.
- [33] J. Pyun, K. Matyjaszewski, *Chem Mater.*, 2001, **13**, 3436-3448.
- [34] Z.Y. Ma, X. Jia, G.X. Zhang, J.M. Hu, X.L. Zhang, Z.Y. Liu, H.Y. Wang, F. Zhou, *J Agr Food Chem.*, 2013, **61**, 5474-5482.
- [35] A.M. Master, M.E. Rodriguez, M.E. Kenney, N.L. Oleinick, A.S. Gupta, *J Pharm Sci-U.S.*, 2010, **99**, 2386-2398.
- [36] Z. Wang, Y. Li, X.-H. Dong, X. Yu, K. Guo, H. Su, K. Yue, C. Wesdemiotis, S.Z. Cheng, W.-B. Zhang, *Chem Sci.*, 2013, **4**, 1345-1352.
- [37] J. Chen, M. Liu, C. Gao, S. Lü, X. Zhang, Z. Liu, *RSC Adv.*, 2013, **3**, 15085-15093.
- [38] C.Y. Zhang, Y.Q. Yang, T.X. Huang, B. Zhao, X.D. Guo, J.F. Wang, L.J. Zhang, *Biomaterials*, 2012, **33**, 6273-6283.
- [39] Y.Q. Yang, B. Zhao, Z.D. Li, W.J. Lin, C.Y. Zhang, X.D. Guo, J.F. Wang, L.J. Zhang, *Acta Biomater.*, 2013, **9**, 7679-7690.
- [40] Y. Cheng, J. Hao, L.A. Lee, M.C. Biewer, Q. Wang, M.C. Stefan, *Biomacromolecules*, 2012, **13**, 2163-2173.
- [41] J. Liu, Y. Xu, Q. Yang, C. Li, W.E. Hennink, R. Zhuo, X. Jiang, *Acta Biomater.*, 2013, **9**, 7758-7766.
- [42] J. Hu, J. He, D. Cao, M. Zhang, P. Ni, *Polym Chem.*, 2015, **6**, 3205-3216.
- [43] Z. Zhang, L. Yin, C. Tu, Z. Song, Y. Zhang, Y. Xu, R. Tong, Q. Zhou, J. Ren, J. Cheng, *ACS Macro Lett.*, 2012, **2**, 40-44.
- [44] Y. Li, J. Lin, X. Yang, Y. Li, S. Wu, Y. Huang, S. Ye, L. Xie, L. Dai, Z. Hou, *ACS Appl Mater Inter.*, 2015, **7**, 17573-17581.
- [45] Y. Liu, X. Yang, W. Zhang, S. Zheng, *Polymer*, 2006, **47**, 6814-6825.
- [46] W. Yuan, T. Shen, X. Liu, J. Ren, *Mater Lett.*, 2013, **111**, 9-12.
- [47] X. Huang, Y. Xiao, M. Lang, *J Colloid Interf Sci.*, 2011, **364**, 92-99.
- [48] Y. Wang, S.M. Grayson, *Adv Drug Deliver Rev.*, 2012, **64**, 852-865.
- [49] Y.Q. Yang, B. Zhao, Z.D. Li, W.J. Lin, C.Y. Zhang, X.D. Guo, J.F. Wang, L.J. Zhang, *Acta Biomater.*, 2013, **9**, 7679-7690.
- [50] J. Hu, S. Liu, *Macromol Chem Phys.*, 2015, **216**, 591-604.
- [51] Li L, Lu B, Wu J, Fan Q, Guo X, Liu Z. *New J Chem.*, 2016, **40**,

Journal Name

COMMUNICATION

4761-4768.

[52] Q. Liu, J. Chen, J. Du, *Biomacromolecules*, 2014, **15**, 3072-3082.[53] M. Zhang, Q. Xiong, J. Chen, Y. Wang, Q. Zhang, *Polym Chem.*, 2013, **4**, 5086-5095.

Illustration of pH-responsive self-assembly of the star-shaped POSS-(PCL-P(DMAEMA-co-PEGMA))₁₆ copolymer for the efficient intracellular release of anti-cancer drugs triggered by the acidic microenvironment inside the tumor tissue.

